

J E P T

Edited by: DGO-Fachausschuss Forschung – Hilden / Germany

Adsorption and inhibitive properties of aqueous extracts of rosmarinus as a green corrosion extract for copper in HNO_3

The efficiency of plant extract as corrosion extract for copper in 1M HNO_3 medium was carried out using weight loss, potentiodynamic polarization, electrochemical impedance spectroscopy (EIS) and electrochemical frequency modulation (EFM) techniques. The results showed variation in inhibition performance of the extract with varying concentration, immersion time and temperature. Langmuir isotherm was tested to describe the adsorption behavior of the extract on the copper surface. Potentiodynamic polarization study clearly revealed that this extract acts as a mixed type inhibitor i.e. the addition of the extract enhances both cathodic and anodic reactions. The results of the electrochemical impedance study showed a decrease in double layer capacitance and an increase in the charge...

Received: 2016-09-19

Received in revised form: 2016-11-15

Accepted: 2016-11-28

Keywords:

Green corrosion, Copper, HNO_3 ,
Rosmarinus extract, Adsorption

Authors:

A.S. Fouda, H.M. Kila,
A.A. Attia, A.M. Salem

DOI:

10.12850/ISSN2196-0267.JEPT5600

Adsorption and inhibitive properties of aqueous extracts of rosmarinus as a green corrosion extract for copper in HNO_3

A.S. Fouda^{1*}, H.M. Kila², A.A. Attia², A.M. Salem²

¹ Chemistry Department, Faculty of Science, Mansoura University, Mansoura-35516, Egypt,

* Email: asfouda@hotmail.com, Fax: +2 050 2202271, Tel: +2 050 2365730

² Chemistry Department, Faculty of Science, Zagazig University, Zagazig, Egypt

The efficiency of plant extract as corrosion extract for copper in 1M HNO_3 medium was carried out using weight loss, potentiodynamic polarization, electrochemical impedance spectroscopy (EIS) and electrochemical frequency modulation (EFM) techniques.

The results showed variation in inhibition performance of the extract with

varying concentration, immersion time and temperature. Langmuir isotherm was tested to describe the adsorption behavior of the extract on the copper surface. Potentiodynamic polarization study clearly revealed that this extract acts as a mixed type inhibitor i.e. the addition of the extract enhances both cathodic and anodic reactions. The results of the electrochemical impedance study showed a decrease in double layer capacitance and an increase in the charge transfer resistance. The results showed that rosmarinus extract could play significant role as corrosion inhibitor for copper in 1M HNO_3 .

Keywords: Green corrosion, Copper, HNO_3 , Rosmarinus extract, Adsorption

Paper: Received: 2016-09-19 / Received in revised form: 2016-11-15 / Accepted: 2016-11-28

DOI: 10.12850/ISSN2196-0267.JEPT5600

1. Introduction

In industries, hydrochloric acid and nitric acid is widely used for acid pickling, acid cleaning and removing rust and decaling acids [1]. Therefore, the corrosion process controls under the influence of acidic conditions are important subjects worthy of intensive research. Most organic substance and plant extracts employed as corrosion inhibitors for copper protect the metal from corrosion by forming a chelate on the metal surfaces [2]. The efficiency of the extract depends on the

stability of the chelate formed [3]. The variation in inhibitive efficiency mainly depends on the type and the nature of the substituents present in the extract molecule [4]. Due to environmental requirements currently imposed environmental corrosion extracts, there is a growing interest in the use of natural products (green corrosion inhibitors) such as extracts of leaves, seeds or bark extracts. These green corrosion inhibitors are biodegradable and do not contain heavy metals or other toxic compounds. Some research groups have reported the successful use of nat-

urally occurring substances to inhibit the corrosion of metals in acidic and alkaline environment. *Delonix regia* extracts inhibited the corrosion of Al in HCl solutions [5], rosemary leaves were studied as corrosion inhibitor for the Al + 2.5 Mg alloy in a 3% NaCl solution at 25°C [6], and El-Etre investigated natural honey as a corrosion inhibitor for Cu [7] and investigated opuntia extract on Al [8]. The inhibitive effect of the extract of khillah seeds on the corrosion of SX 316 steel in HCl solution was determined. The mechanism of action is attributed to the formation of insoluble complexes as a result of interaction between iron cations, and khillah [9]. Ebenso et al. showed the inhibition of corrosion with ethanolic extract of African bush pepper (*Piper guinensis*) on mild steel [10]; *Carica papaya* leaves extract [11]; neem leaves extract (*Azadirachta indica*) on mild steel in H₂SO₄ [12]. Zucchi and Omar investigated plant extracts of *Papaia*, *Poinciana pulcherrima*, *Cassia occidentalis*, and *Datura stramonium* seeds and *Papaya*, *Calotropis procera* B, *Azadirachta indica*, and *Auforpio turkiale* sap for their corrosion inhibition potential and found that all extracts except those of *Auforpio turkiale* and *Azadirachta indica* reduced the corrosion of steel with an efficiency of 88%–96% in 1 N HCl and with a slightly lower efficiency in 2 N HCl. They attributed the effect to the products of the hydrolysis of the protein content of these plants [13]; Umoren et al. [14] studied the corrosion inhibition of mild steel in H₂SO₄ in the presence of gum arabic (GA) (naturally occurring polymer) and polyethylene glycol (PEG) (synthetic polymer). It was found that PEG was more effective than gum arabic. Fouda et al. investigated the effect of *Melilotus officinalis* Extract (MOE), as a green corrosion inhibitor

for Al in 1 M HCl [15], *Adhatoda* aqueous plant extract as Corrosion inhibitor for carbon steel in sanitation water in polluted NaCl solutions [16], *Roselle* extract [17] and *Thevetia peruviana* as corrosion inhibitors for carbon steel in HCl solution [18]. Some other authors reported the use of natural products in the development of green corrosion extracts as effective for different metals in various environments [18–24].

The aim of this work is to study the corrosion inhibition of copper in 1 M HNO₃ using *rosmarinus* extract as green corrosion inhibitor by chemical and electrochemical measurements.

2. Experimental Method

2.1 Materials and solutions

Table 1 shows the chemical composition of the tested copper in chemical and electrochemical methods

The experimental measurements were carried out in 1 M HNO₃ solution in the absence and presence of various concentrations of *rosmarinus* extract

2.2 Methods used for corrosion measurements

2.2.1 Weight loss measurements

For weight loss measurements, square specimens of size 2 x 2 x 0.2 cm were used. The specimens were first abraded to a mirror finish using different grades (320–1200 grade) of emery papers,

Element	Sn	Ag	Fe	Bi	Pb	As	Cu
Weight %	0.001	0.001	0.01	0.0005	0.002	0.0002	The rest

Tab. 1: Chemical composition of used copper in weight %

decreased with acetone, washed with bidistilled water and dried with soft paper before weighed. The weight loss measurements were carried out in a 100 ml capacity glass beaker placed in water thermostated bath. The specimens were then immediately immersed in the test solution without or with desired concentration of the investigated plant extract. Triplicate specimens were exposed for each condition and the mean weight losses were reported in order to verify reproducibility of the experiments. The inhibition efficiency (IE) and the degree of surface coverage (θ) of the investigated extract on corrosion of copper were calculated using equation (1) [25]:

$$\%IE = \theta \times 100 = [1 - (W/W^0)] \times 100 \quad (1)$$

Where W and W^0 are the weight losses in the presence and absence of the extract, respectively.

2.2.2. Electrochemical Measurements

Polarization experiments were carried out in a conventional three-electrode cell with a platinum counter electrode (1 cm^2) and a saturated calomel electrode (SCE) coupled to a fine Luggin capillary (to minimize the IR resistance) as the reference electrode. The working electrode was in the form of a square cut from copper embedded in epoxy resin of polytetrafluoroethylene (PTFE) so that the flat surface was the only surface in the electrode. The working electrode was immersed in the test solution before starting the measurements, until a steady state was reached (30 min). For potentiodynamic polarization measurements, the potential was scanned at a scan rate of 1 mVs^{-1} . Potential changed automatically from -0.600 to 1 V vs SCE. EIS measurements were performed at open circuit potential over a frequency range of 0.1 Hz to 100 kHz . The sinusoidal potential perturbation was 5 mV in amplitude. EFM carried out using two frequencies 2.0 and 5.0 Hz . The

base frequency was 1.0 Hz . We use a perturbation signal with amplitude of 10 mV for both perturbation frequencies of 2.0 and 5.0 Hz .

The electrochemical measurements were carried out using a Gamry instrument Potentiostat/Galvanostat/ZRA (PCI300/4). This includes a Gamry Framework system based on the ESA400, Gamry applications that include DC105 for dc corrosion measurements, EIS300 software for electrochemical impedance spectroscopy and EFM140 software for electrochemical frequency modulation measurements along with a computer for collecting data. Electrochemical data were analyzed by Echem Analyst 5.5 software.

2.2.3 Scanning electron microscopy measurements (SEM)

The electron surface of copper was examined by scanning electron microscope- type JOEL 840, Japan before and after immersion in 1 M HNO_3 test solution in the absence and presence of the optimum concentration of the investigated extract at 25°C , for 2 days immersion time. The specimens were washed gently with bidistilled water, then dried carefully and examined without any further treatments.

3. Results and Discussion

3.1. Chemical method (Weight loss method)

Weight-loss of copper was determined, at various time intervals, in the absence and presence of different concentrations of the extract. The obtained weight loss-time curves are represented in Figure 1 for rosmarinus extract. The inhibition efficiency of corrosion was found to be dependent on the extract concentration (Table 2). The curves obtained in the presence of extract fall significantly below that of free acid. In all cases,

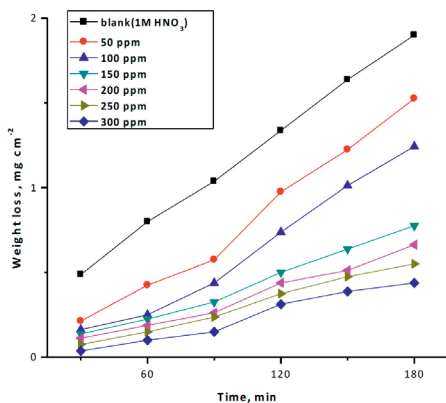


Fig. 1: Weight loss-time curves for the corrosion of copper in 1 M HNO_3 in the absence and presence of different concentrations of rosmarinus extract at 25°C

Conc. of inhibitor $\times 10^6$ M	% IE	θ
1	27.1	0.271
3	44.8	0.448
5	62.6	0.626
7	67.2	0.672
9	72.0	0.720
11	77.0	0.770

Tab. 2: Values of inhibition efficiencies (% IE) and surface coverage (θ) of extract for the corrosion of copper in 1 M HNO_3 from weight loss measurements at different concentrations and at 25°C

Conc. of inhibitor $\times 10^6$ M	298		303K		308K		313K		318K	
	C.R	%IE								
1	8.12	27.1	10.2	55.0	10.5	67.2	12.3	71.1	13.3	75.0
3	6.14	44.8	9.16	59.0	9.27	71.4	11.2	74.0	11.4	78.6
5	4.16	62.6	6.04	73.2	8.33	74.0	8.64	80.0	10.2	81.0
7	3.33	67.3	4.79	79.0	6.45	80.0	7.29	83.0	8.12	85.0
9	3.12	72.0	4.16	82.0	5.52	83.0	6.04	86.0	6.77	87.3
11	2.60	77.0	3.64	84.0	5.00	84.4	5.62	87.0	5.41	90.0

Table 3: Values of inhibition efficiencies %IE and corrosion rate (C.R) of rosmarinus extract for the corrosion of copper in 1 M HNO_3 from weight-loss measurements at different concentrations at temperature range of 298-313 K.

the increase in the extract concentration was accompanied by a decrease in weight-loss and an increase in the percentage inhibition. These results lead to the conclusion that rosmarinus extract under investigation is fairly efficient as extract for copper dissolution in nitric acid solution. Also, the degree of surface coverage (θ) by the extract was found to increase with increasing the extract concentration.

3.2. Effect of Temperature

The effect of temperature on the corrosion rate of copper in 1M HNO_3 and in presence of different extract concentrations was studied in the temperature range of 298–313K using weight loss measurements. As the temperature increases, the rate of corrosion decreases and the inhibition efficiency of the extract increases as shown in Table 3 for rosmarinus extract. The adsorption behavior of extract on copper surface occurs through chemical adsorption.

3.3. Adsorption isotherms

One of the most convenient ways of expressing adsorption quantitatively is by deriving the adsorption isotherm that characterizes the metal/extract/ environment system. Various adsorption

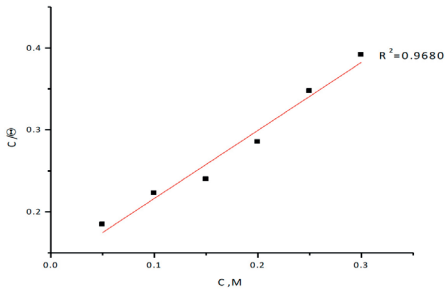


Fig. 2: Langmuir adsorption isotherm plotted as C/θ vs C of Rosmarinus extract for corrosion of copper in 1M HNO_3 solution from weight loss method at 25°C

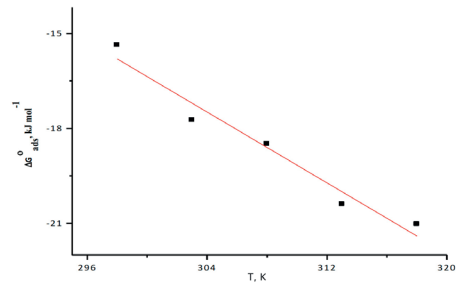


Fig. 3: Variation of $\Delta G_{\text{ads}}^{\circ}$ versus T for the adsorption of extract on copper surface in 1 M HNO_3 at different temperatures

isotherms were applied to fit θ values, but the best fit was found to obey Langmuir adsorption isotherm which are represented in Figure 2 for Rosmarinus extract, Langmuir adsorption isotherm may be expressed by Equation (2):

$$C/\theta = 1/K_{\text{ads}} + C \quad (2)$$

Where C is the concentration (mL/L) of the extract in the bulk electrolyte, K_{ads} is the adsorption equilibrium constant. A plot of θ versus C/θ should give straight lines. In order to get a comparative view, the variation of the adsorption equilibrium constant (K_{ads}) of the extract with its molar concentration was calculated. The experimental data give good curve fitting for the applied adsorption isotherm as the correlation coefficients (R^2) were

close to unity. The extent of inhibition is directly related to the performance of adsorption layer which is sensitive function of a molecular structure. The equilibrium constant of adsorption K_{ads} obtained from the intercepts of Langmuir adsorption isotherm is related to the free energy of adsorption $\Delta G_{\text{ads}}^{\circ}$ as follows:

$$K_{\text{ads}} = 1/55.5 \exp(-\Delta G_{\text{ads}}^{\circ}/RT) \quad (3)$$

where, the value 55.5 is the concentration of water on the metal surface in mol/L. Plot of ($\Delta G_{\text{ads}}^{\circ}$) versus T (Fig. 3) gave the heat of adsorption ($\Delta H_{\text{ads}}^{\circ}$) and the entropy ($\Delta S_{\text{ads}}^{\circ}$) according to the thermodynamic basic Equation (4):

$$\Delta G_{\text{ads}}^{\circ} = \Delta H_{\text{ads}}^{\circ} - T\Delta S_{\text{ads}}^{\circ} \quad (4)$$

Temp., °C	$K_{\text{ads}} \times 10^{-3}$ M^{-1}	Slope	$-\Delta G_{\text{ads}}^{\circ}$ kJ mol^{-1}	$\Delta H_{\text{ads}}^{\circ}$ kJ mol^{-1}	$\Delta S_{\text{ads}}^{\circ}$ $\text{J mol}^{-1} \text{K}^{-1}$
25	8.868	0.9181	25.4	77.6	278.4
30	20.533	1.0437	27.7		281.6
35	37.152	1.107	29.5		282.9
40	45.599	1.0833	30.4		281.1
45	51.177	1.0648	31.0		278.7

Tab. 4: Adsorption parameters for Rosmarinus extract in 1 M HNO_3 obtained from Langmuir adsorption isotherm at different temperatures

Table 4 clearly shows a good dependence of $\Delta G_{\text{ads}}^{\circ}$ on T, indicating the good correlation among thermodynamic parameters. The negative value of $\Delta G_{\text{ads}}^{\circ}$ reflects that the adsorption of studied extract on copper surface from 1 M HNO_3 solution is spontaneous process and stability of the adsorbed layer on copper surface. Generally, values of $\Delta G_{\text{ads}}^{\circ}$ around -20 kJ mol^{-1} or lower are consistent with the electrostatic interaction between the charged molecules and the charged metal (physical adsorption); those around -40 kJ mol^{-1} or higher involves formation of coordinate bond (chemisorption) [26]. The calculated $\Delta G_{\text{ads}}^{\circ}$ values are in between -20 and -40 kJ mol^{-1} indicating that the adsorption mechanism of the extract on copper in 1 M HNO_3 solutions was typical comprehensive of physical and chemical adsorption.

Plot of $(\Delta G_{\text{ads}}^{\circ})$ versus T Figure 3 gave the heat of adsorption $(\Delta H_{\text{ads}}^{\circ})$ and the standard entropy $(\Delta S_{\text{ads}}^{\circ})$ according to the thermodynamic basic Equation (5):

$$\Delta G_{\text{ads}}^{\circ} = \Delta H_{\text{ads}}^{\circ} - T \Delta S_{\text{ads}}^{\circ} \quad (5)$$

The values of thermodynamic parameter for the adsorption of extract Table 4 can provide valuable information about the mechanism of corrosion inhibition. While an endothermic adsorption process $(\Delta H_{\text{ads}}^{\circ} > 0)$ is attributed unequivocally to an exothermic adsorption process $(\Delta H_{\text{ads}}^{\circ} < 0)$ may involve either exothermic adsorption or endothermic adsorption or mixture of both processes. In the presented case, the calculated positive values of $\Delta H_{\text{ads}}^{\circ}$ for the adsorption of extract in 1 M HNO_3 indicating that Rosmarinus extract may be chemically adsorbed. The $\Delta S_{\text{ads}}^{\circ}$ values in the presence of extract in 1 M HNO_3 are positive. This indicates that an increase in disorder takes places on going from reactants to the metal-adsorbed reaction complex [27].

3.4. Kinetic –thermodynamic corrosion parameters

The activation parameters for the corrosion process were calculated from Arrhenius-type plot according to Equation (6):

$$k_{\text{corr}} = A \exp(E_a^*/RT) \quad (6)$$

Where E_a^* is the apparent activation corrosion energy, R is the universal gas constant, T is the absolute temperature and A is the Arrhenius pre-exponential constant. Values of apparent activation energy of corrosion for copper in 1 M HNO_3 shown in Table 5, without and with various concentrations of Rosmarinus extract determined from the slope of $\log(k_{\text{corr}})$ versus $1/T$ plots are shown in Figure 4. Inspection of the data shows that the activation energy is lower in the presence of extract than in its absence. This was attributed to slow rate of extract adsorption with a resultant closer approach to equilibrium during the experiments at higher temperatures according to Hoar and Holliday [28]. But, Riggs and Hurd [29] explained that the decrease in the activation energy of corrosion at higher levels of inhibition arises from a shift of the net corrosion reaction from the uncovered part of the metal surface to

Conc. of inhibitor $\times 10^6 \text{ M}$	E_a^* kJ mol^{-1}	ΔH^* kJ mol^{-1}	$-\Delta S^*$ $\text{J mol}^{-1}\text{K}^{-1}$
0	55.5	56.6	90.9
1	24.7	34.5	170.9
3	23.6	33.5	176.2
5	23.2	33.1	179.4
7	21.7	31.3	186.6
9	21.1	30.9	190.0
11	19.1	30.5	192.8

Tab. 5: Activation parameters for copper corrosion in the absence and presence of various concentrations of Rosmarinus extract in 1 M HNO_3

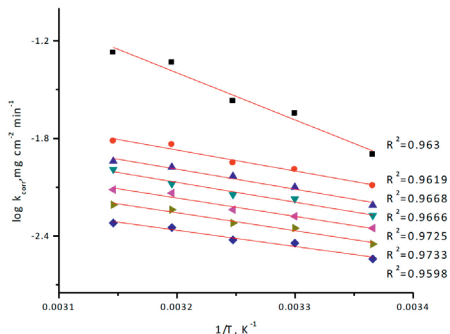


Fig. 4: Arrhenius plots for copper corrosion rates (k_{corr}) after 120 minute of immersion in 1 M HNO_3 in the absence and presence of various concentrations of rosmarinus extract

the covered one. Schmid and Huang [30] found that organic molecules inhibit both the anodic and cathodic partial reactions on the electrode surface and a parallel reaction takes place on the covered area, but the reaction rate on the covered area is substantially less than on the uncovered area similar to the present study. The alternative formulation of transition state equation is shown in Equation (7):

$$k_{\text{corr}} = (RT/Nh) \exp(\Delta S^*/R) \exp(-\Delta H^*/RT) \quad (7)$$

Where k_{corr} is the rate of metal dissolution, h is Planck's constant, N is Avogadro's number, ΔS^* is the entropy of activation and ΔH^* is the enthalpy of activation. Figure 5 shows a plot of $\log k/T$ against $(1/T)$ in 1 M HNO_3 . Straight lines are obtained with slopes equal to $(\Delta H^*/2.303R)$ and intercepts are $[\log(R/Nh + \Delta S^*/2.303R)]$ are calculated and their values are listed in Table 5.

The increase in E_a^* with increase extract concentration Table 5 is typical of physical adsorption. The positive signs of the enthalpies (ΔH^*) reflect the endothermic nature of the copper dissolution process. Value of entropies (ΔS^*) imply that the

activated complex at the rate determining step represents an association rather than a dissociation step, meaning that a decrease in disordering takes place on going from reactants to the activated complex [31,32].

3.5. Potentiodynamic polarization measurements

Figure 6 shows typical polarization curves for copper in 1 M HNO_3 solution. The two distinct regions that appeared were the active dissolution region (apparent Tafel region), and the limiting current region. In the extract-free solution, the anodic polarization curve of copper showed a monotonic increase of current with potential until the current reached the maximum value. After this maximum current density value, the current density declined rapidly with potential increase, forming an anodic current peak that was related to $\text{Cu}(\text{NO}_3)_2$ film formation. In the presence of extract, both the cathodic and anodic current densities were greatly decreased over a wide potential range. Various corrosion parameters such as corrosion potential (E_{corr}), anodic and cathodic Tafel slopes (β_a , β_c), the corrosion cur-

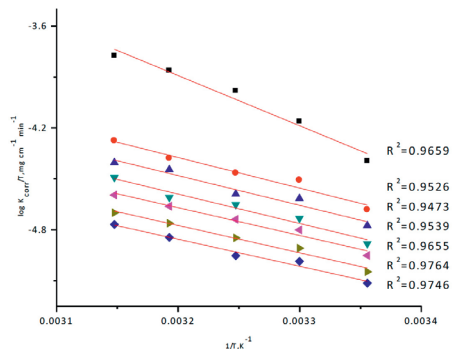


Fig. (5): Transition-state for copper corrosion rates (k_{corr}/T) in 1 M HNO_3 in the absence and presence of various concentrations of Rosmarinus extract

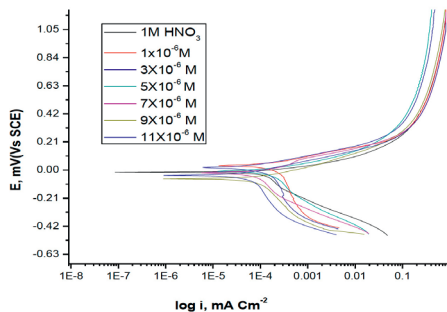


Fig. 6: Potentiodynamic polarization curves for the dissolution of copper in 1M HNO₃ in absence and presence of different concentrations of Rosmarinus extract at 25°C

rent density (i_{corr}), the degree of surface coverage (θ) and the inhibition efficiency (%IE) are given in Table 6. It can be seen from the experimental results that in all cases, addition of extract induced a significant decrease in cathode and anodic currents. The values of E_{corr} were affected and slightly changed by the addition of extract. This indicates that chenopodium extract acts as mixed-type extract. The slopes of anodic and cathodic Tafel lines (β_a and β_c), were slightly changed (Tafel lines are parallel), on increasing the concentration of chenopodium extract which indicates that there is no change of the mechanism of inhibition in

the presence and absence of extract. The orders of inhibition efficiency of extract at different concentrations as given by polarization measurements are listed in Table 6. The results are in good agreement with those obtained from weight-loss measurements. The inhibition efficiencies %IE_{EFM} increase by increasing the inhibitor concentrations and was calculated as from Equation (8):

$$\%IE_{EFM} = [1 - (i_{corr}/i_{corr}^0)] \times 100 \quad (8)$$

Where i_{corr}^0 and i_{corr} are corrosion current densities in the absence and presence of Rosmarinus extract.

3.6. Electrochemical impedance spectroscopy (EIS) measurements

EIS is well-established and it is a powerful technique for studying corrosion. Surface properties, electrode kinetics and mechanistic information can be obtained from impedance diagrams [33-37]. Figure 7 shows the Nyquist (a) and Bode (b) plots obtained at open-circuit potential both in the absence and presence of increasing concentration of Rosmarinus extract at 25°C. The increase in the size of the capacitive loop with the addition of extract shows that a barrier grad-

	Conc. of extract $\times 10^6$ M	$-E_{corr}$ mV vs SCE	$i_{corr} \times 10^{-4}$ $\mu A cm^{-2}$	β_a mV dec ⁻¹	β_c mV dec ⁻¹	C.R. mpy	% IE	θ
Blank	0	16	512.0	218	222	252.6	----	----
rosmarinus extract	1	45	66.40	72	207	32.75	86.7	0.867
	3	39	65.80	71	189	32.47	87.1	0.871
	5	43	64.70	75	198	31.92	87.4	0.874
	7	49	37.60	59	203	18.56	92.6	0.926
	9	89	33.50	100	228	16.53	93.5	0.935
	11	83	28.00	71	217	13.83	94.5	0.945

Tab. 6: Corrosion potential (E_{corr}), corrosion current density (i_{corr}), Tafel slopes (β_a , β_c), degree of surface coverage (θ) and inhibition efficiency (%IE) of copper in 1M HNO₃ at 25°C for Rosmarinus extract

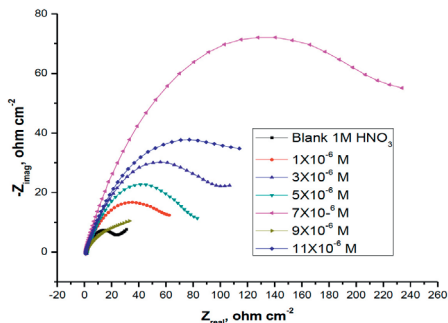


Fig. 7a: The Nyquist plots for corrosion of copper in 1M HNO₃ in the absence and presence of different concentrations of Rosmarinus extract at 25°C

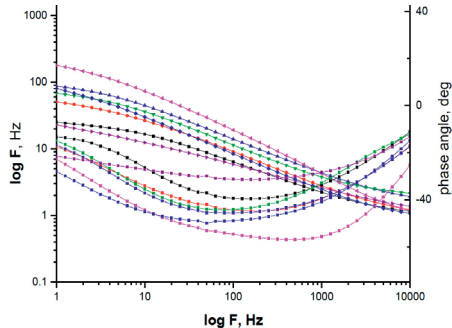


Fig. 7b: The Bode plots for the corrosion of copper in 1M HNO₃ in the absence and presence of different concentrations of Rosmarinus extract at 25°C

ually forms on the copper surface. The increase in the capacitive loop size (Figure 7a) enhances, at a fixed extract concentration, following the order. Bode plots (Figure 7b), shows that the total impedance increases with increasing extract concentration ($\log Z$ vs. $\log f$). But ($\log f$ vs. phase), also Bode plot shows the continuous increase in the phase angle shift, obviously correlating with the increase of extract adsorbed on copper surface. The Nyquist plots do not yield perfect semicircles as expected from the theory of EIS. The deviation from ideal semicircle was generally attributed to the frequency dispersion

[38] as well as to the inhomogenities of the surface. EIS spectra of the investigated extract were analyzed using the equivalent circuit, Figure 8, which represents a single charge transfer reaction and fits well with our experimental results.

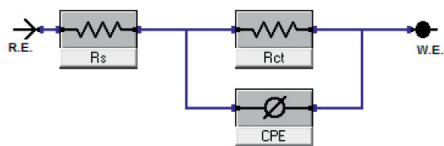


Fig. 8: Equivalent circuit model used to fit experimental EIS

Extract	Conc. of inhibitor $\times 10^6$ M	R_{ct} , $\Omega \text{ cm}^2$	$R_s \times 10^{-3}$, $\Omega \text{ cm}^2$	$C_{dl} \times 10^{-4}$, $\mu\text{F cm}^2$	% IE	θ
Blank	0	28.60	968.1	6.045	-----	-----
Rosmarinus extract	1	39.35	982.6	2.800	27.3	0.273
	3	63.98	910.5	5.830	55.3	0.553
	5	84.22	1778	4.45	66.0	0.660
	7	112.5	1463	3.83	74.6	0.746
	9	134.2	844.1	9.72	78.7	0.787
	11	231.3	827.4	2.41	87.6	0.876

Tab. 7: Electrochemical kinetic parameters obtained by EIS technique for in 1 M HNO₃ without and with various concentrations of Rosmarinus extract at 25°C

The constant phase element, CPE, is introduced in the circuit instead of a pure double layer capacitor to give a more accurate fit [39]. The double layer capacitance, C_{dl} , for a circuit including a CPE parameter (Y_0 and n) was calculated from Equation 9 [40]:

$$C_{dl} = Y_0 (\omega_{max})^{n-1} \quad (9)$$

where Y_0 is the magnitude of the CPE, $\omega_{max} = 2\pi f_{max}$, f_{max} is the frequency at which the imaginary component of the impedance is maximal and the factor n is an adjustable parameter that usually lies between 0.50 and 1.0. After analyzing the shape of the Nyquist plots, it is concluded that the curves approximated by a single capacitive semicircles, showing that the corrosion process was mainly charge-transfer controlled [41, 42]. The general shape of the curves is very similar for all samples (in presence or absence of extract at different immersion times) indicating that no change in the corrosion mechanism [43]. From the impedance data Table 7, we concluded that the value of R_{ct} increases with increasing the concentration of the extract and this indicates an increase thickness of the barrier layer formed on copper surface. In fact the presence of extracts enhances the value of R_{ct} in acidic solution. Values of double layer capacitance are also brought down to the maximum extent in the presence of extract and the decrease in the values of CPE follows the order similar to that obtained for i_{corr} in this study. The decrease in CPE/C_{dl} results from a decrease in local dielectric constant and/or an increase in the thickness of the double layer, suggesting that organic derivatives inhibit the copper corrosion by adsorption at metal/acid [44, 45]. The inhibition efficiency was calculated from the charge transfer resistance data from Equation 10 [46]:

$$\% IE_{EIS} = [1 - (R_{ct}^0 / R_{ct})] \times 100 \quad (10)$$

where R_{ct}^0 and R_{ct} are the charge-transfer resistance values without and with extract, respectively.

3.7. Electrochemical frequency modulation (EFM) measurements

EFM is a nondestructive corrosion measurement technique that can directly and quickly determine the corrosion current values without prior knowledge of Tafel slopes, and with only a small polarizing signal. These advantages of EFM technique make it an ideal candidate for online corrosion monitoring [45]. The great strength of the EFM is the causality factors which serve as an internal check on the validity of EFM measurement. The causality factors CF-2 and CF-3 are calculated from the frequency spectrum of the current responses. The experimental EFM data were treated using two different models: complete diffusion control of the cathodic reaction and the "activation" model. For the latter, a set of three non-linear equations had been solved, assuming that the corrosion potential does not change due to the polarization of the working electrode [46]. The larger peaks were used to calculate the corrosion current density (i_{corr}), the Tafel slopes (β_c and β_a) and the causality factors (CF-2 and CF-3). These electrochemical parameters were listed in Table 8. The data presented in Table 8 obviously show that, the addition of Rosmarinus extract at a given concentration to the acidic solution decreases the corrosion current density, indicating that this compound inhibits the corrosion of copper in 1 M HNO_3 through adsorption. The causality factors obtained under different experimental conditions are approximately equal to the theoretical values (2 and 3) indicating that the measured data are verified and of good quality. The inhibition efficiencies %IEEFM increase by increasing the extract concentrations and was calculated as from Equation (8).

Conc. of inhibitor $\times 10^6$ M	i_{corr} $\mu\text{A cm}^{-2}$	β_a mVdec^{-1}	β_c mVdec^{-1}	CF-2	CF-3	C.R mpy	θ	% IE
0	523.7	64	193	2.325	3.700	258.5	----	----
1	360.8	60	277	1.968	4.007	178.1	0.485	48.5
3	215.7	60	110	2.009	4.019	106.4	0.706	70.6
5	208.4	58	295	1.999	3.990	102.8	0.711	71.1
7	107.7	40	164	2.036	4.614	53.15	0.794	79.4
9	89.95	64	169	1.823	3.780	44.39	0.828	82.8
11	63.02	46	197	1.927	2.741	28.80	0.788	78.8

Tab. 8: Electrochemical kinetic parameters obtained by EFM technique for copper in the absence and presence of various concentrations of chenopodium extract in 1M HNO_3 at 25°C

3.8. Surface examination

In order to verify if the Rosmarinus extract molecules are in fact adsorbed on copper surface, SEM experiments were carried out. The SEM micrographs for copper surface alone and after 48 h immersion in 1 M HNO_3 without and with the addition of 11×10^{-6} M of Rosmarinus extract are shown in Figures (9a-c). As expected, Figure 9a shows metallic surface is clear, while in the absence of extract, the copper surface is damaged by HNO_3 corrosion (Figure 9b). In contrast, in presence of the investigated extract (Figure 9c); the metallic surface seems to be almost no affected by corrosion. The formation

of a thin film of chenopodium extract observed in SEM micrograph, thus protecting the surface against corrosion.

3.9. Mechanism of corrosion inhibition

Results of the present study have shown that Rosmarinus extract inhibits the acid induced corrosion of copper by virtue of adsorption of its components (major components [47] were α -pinene (40.55 to 45.10%), 1,8-cineole (17.40 to 19.35%), camphene (4.73 to 6.06%) and verbenone (2.32 to 3.86%) onto the metal surface. The inhibition process is a function of the metal, extract concentration, and temperature as well

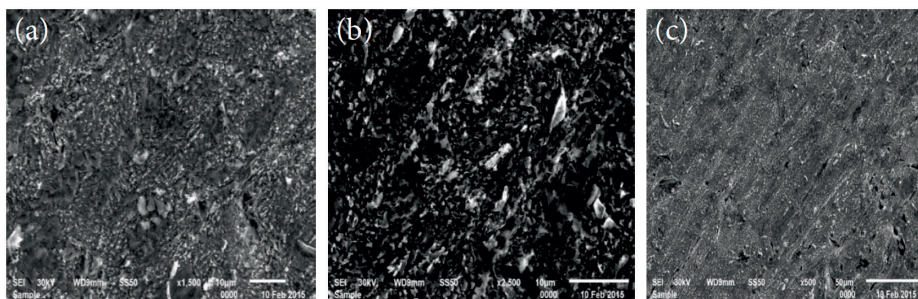


Fig. 9(a-c): SEM micrographs of copper surface (a) before of immersion in 1 M HNO_3 , (b) after 48 h of immersion in 1 M HNO_3 , (c) after 48 h of immersion in 1 M HNO_3 + 11×10^{-6} M of Rosmarinus extract at 25°C.

as inhibitor adsorption abilities which is so much dependent on the number of adsorption sites. The mode of adsorption (physisorption and chemisorption) observed could be attributed to the fact that Rosmarinus contains many different chemical compounds which some can adsorbed chemically and others adsorbed physically. This observation may be attributed to the fact that adsorbed organic molecules can influence the behavior of electrochemical reactions involved in corrosion processes in several ways. The action of organic inhibitors depends on the type of interactions between the substance and the metallic surface. The interactions can bring about a change either in electrochemical mechanism or in the surface available for the processes [48].

4. Conclusions

From the results of the study the following may be concluded:

1. Rosmarinus extract is good corrosion extract for copper in 1 M HNO_3 solution.
2. Reasonably good agreement was observed between the values obtained from the weight loss and electrochemical measurements.
3. Results obtained from potentiodynamic polarization indicated that Rosmarinus extract is mixed-type inhibitor
4. Percentage inhibition efficiency of Rosmarinus extract was temperature dependent and its addition led to a decrease of the activation corrosion energy.
5. The thermodynamic parameters revealed that the inhibition of corrosion by Rosmarinus extract is due to the formation of a chemical adsorbed film on the metal surface.
6. The adsorption of Rosmarinus extract onto copper surface follows the Langmuir adsorption isotherm model.

References

- [1] M.Scendo, Corros. Sci., 49 (2007) 3953.
- [2] M.Duprat, N.Bui, F.Dabost, Corrosion 35 (1979) 392.
- [3] J.M.Costa, Lluçh J.M., Corrosion Science 24 (1984) 929.
- [4] B.Dus, Z.S.Smialowska, Corrosion 28 (1972) 105.
- [5] O. K. Abiola, N. C. Oforika, E. E. Ebenso, and N. M. Nwinuka, Anti-Corrosion Methods and Materials, 54(4) (2007) 219–224.
- [6] M. Kliskic, J. Radoservic, S. Gudic, and V. Katalinic, Journal of Applied Electrochemistry, 30(7) (2000) 823–830.
- [7] A. Y. El-Etre, Corros.Sci. 40(11), (1998) 1845–1850.
- [8] A. Y. El-Etre, Corros. Sci, 45(11) (2003) 2485–2495.
- [9] A. Y. El-Etre, Appl. Surf. Sci., vol. 252(24) (2006) 8521–8525.
- [10] E. E. Ebenso, U. J. Iboke, U. J. Ekpe et al., Transactions of the SAEST, 39(4)(2004) 117–123.
- [11] E. E. Ebenso and U. J. Ekpe, West African Journal of Biological and Applied Chemistry, 41(1996) 21–27.
- [12] U. J. Ekpe, E. E. Ebenso, and U. J. Iboke, West African Journal of Biological and Applied Chemistry, 37(1994) 13–30.
- [13] F. Zucchi and I. H. Omar, 24(4) (1985)391–399.
- [14] S. A. Umoren, O. Ogbobe, I. O. Igwe, and E. E. Ebenso, 50(7), (2008) 1998–2006.
- [15] A.S. Fouda, R. Abo-Shohba, W. M. Husien & E. S. Ahmed, Global Journal of Researches in Engineering: C Chemical Engineering, 15(3) (2015) 9-24.
- [16] A.S.Fouda, A. Y. El-Khateeb, M. Ibrahim3 and M.Fakih, Nature and Science 13(2) (2015) 71-82.
- [17] A. A. Nazeer, K. Shalabi, A. S. Fouda, Res Chem Intermed 41(2015)4833–4850.
- [18] A. S. Fouda, H. E. Megahed, N. Fouad, N. M. Elbahrawi, J Bio Tribol Corros. Acta, 31(4) (2016) 1-13.
- [19] I.H. Faroouqi, A. Hussain, P.A. and Quarishi Saini, Anti-Corros., Meth. Mater. 46 (1999) 328.
- [20] S. Martinez and I.Stern, J. Appl. Electrochem., 31(2001) 973.
- [21] A., B Chetouani and M. Hammouti Benkaddour, pigm. Resin Technol., 33 (2004) 26.
- [22] F. Bensabah, S. Houbairi, M.Essahli, A. Lamiri, Naja J., Port. Electrochim. Acta, 31(4) (2013) 195-206.
- [23] L.Valek and S. Martinez, Mater. Lett, 61 (2007) 148.
- [24] OK. Abiola, NC Oforika, EE and NM ebenso Nwinuka, Anti-Corros. Mater, 54(2007) 219.
- [25] AM .Abdel-Gaber, BA. Abd-El-Nabey and M .Saadawy., Corros. Sci., 51(2009) 1038.
- [26] G.N. Mu, , T.P. Zhao, , , M. Liu, T. Gu, , Corrosion 52, (1996) 853.
- [27] A. Yurt, G. Bereket, A. Kivrak, A. Balaban and B. Erk, J Appl Electrochem, 35(2005).
- [28] G. Banerjee & S N. Malhotra, Corrosion. 48, (1992) 10.
- [29] T P. Hour & R D. Holliday, J Appl Chem., 3(1953) 502.

- [30] L O (Jr). Riggs & T J. Hurd, *Corrosion*, 23 (1967) 252.
- [31] G M. Schmid & H J. Huang, *Corros Sci.*, 20 (1980) 1041.
- [32] F. Bentiss, M. Lebrini & M. Lagrenee, *Corros Sci.*, 47 (2005) 2915.
- [33] J. Marsh, *Advanced Organic Chemistry*, 3rd edn (Wiley Eastern, New Delhi), (1988).
- [34] D.C. Silverman and J. E.Carrico, *Corrosion*, 44 (1988) 280.
- [35] W. J.Lorenz and F. Mansfeld, *Corros.Sci.* 21 (1981) 647.
- [36] D. D. Macdonald, M. C. Mckubre., "Impedance measurements in Electrochemical systems," *Modern Aspects of Electrochemistry*, J.O'M. Bockris, B.E. Conway, R.E.White, Eds., Plenum Press, New York, New York, 14(1982) 61.
- [37] F. Mansfeld; *Corrosion*. 36 (1981) 301.
- [38] C. Gabrielli, "Identification of Electrochemical processes by Frequency Response Analysis," *Solarton Instrumentation Group*, (1980).
- [39] M. El Achouri, S. Kertit, H.M. Gouttaya, B. Nciri , Y. Bensouda, L. Perez , M.R. Infante, K. Elkacemi, *Prog. Org. Coat.* 43 (2001) 267.
- [40] J.R. Macdonald, W.B. Johanson, in: J.R. Macdonald (Ed.), *Theory in Impedance Spectroscopy*, John Wiley& Sons, New York, (1987).
- [41] S. F. Mertens, C. Xhoffer, B. C. Decooman, E. Temmerman, *Corrosion*. 53 (1997) 381.
- [42] G. Trabaneli, C. Montecelli, V. Grassi, A. Frignani, *J. Cem. Concr., Res.* 35 (2005)1804.
- [43] F. M. Reis, H.G. De Melo and I.Costa, *Electrochim. Acta.* 51 (2006) 17.
- [44] M. Lagrenee, B. Mernari, M. Bouanis, M. Traisnel & F. Bentiss, *Corros. Sci.* 44 (2002), 573.
- [45] Ma H., Chen S., Niu L., Zhao S., Li S., Li D., *J. Appl. Electrochem.* 32(2002) 65.
- [46] G. A. Caignan, S. K. Metcalf , E. M.Holt, *J.Chem. Cryst.* 30 (2000) 415.
- [47] B.M. Lawrence *Progress in essential oils: rosemary oil. Parfum. Flavor.* 20(1) (1995) 47.
- [48] K. Aramaki,, N. J Hackermann. *Electrochem. Soc.*1969, 116, 568-571.

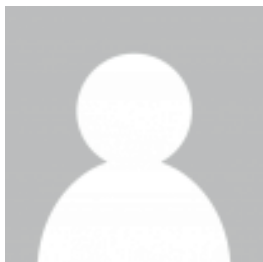
Authors



Prof. Dr. A. S. Fouda
Department of Chemistry, Faculty of Science,
El-Mansoura University
El-Mansoura-35516, Egypt
Email: asfouda@hotmail.com; asfouda@mans.edu.eg
Phone: +2 050 2365730
Fax: +2 050 2246254



H.M. Kila
Department of Chemistry, Faculty of Science,
Zagazig University
Zagazig, Egypt



A.A. Attia
Department of Chemistry, Faculty of Science,
Zagazig University
Zagazig, Egypt



A.M. Salem
Department of Chemistry, Faculty of Science,
Zagazig University
Zagazig, Egypt

CONTACT:

EUGEN G. LEUZE VERLAG KG
Ralf Schattmaier
Karlstraße 4
88348 Bad Saulgau
Germany

Email: ralf.schattmaier@leuze-verlag.de
Phone: +49 0 7581 4801-12
Fax: +49 0 7581 4801-10